4 August 2000

ELSEVIER

Chemical Physics Letters 325 (2000) 619–626

CHEMICAL PHYSICS LETTERS

www.elsevier.nl/locate/cplett

# Temperature dependence of solute vibrational relaxation in supercritical fluids: experiment and theory

D.J. Myers [a], Motoyuki Shigeiwa [a], C. Stromberg [a], M.D. Fayer [a,*], Binny J. Cherayil [b]

[a] *Department of Chemistry, Stanford University, Stanford, CA 94305, USA*
[b] *Department of Inorganic & Physical Chemistry, Indian Institute of Science, Bangalore-560034, India*

Received 7 April 2000; in final form 2 June 2000

**Abstract**

Vibrational lifetime ($T_1$) data for the asymmetric CO stretching mode of $W(CO)_6$ in supercritical ethane and carbon dioxide as a function of temperature at various fixed densities are compared to a recent extended hydrodynamic theory [1]. In ethane at the critical density, as the temperature is raised, $T_1$ initially becomes longer, reaching a maximum $\sim 70$ K above the critical temperature. $T_1$ decreases with further increase in temperature. The theory is able to reproduce this behavior nearly quantitatively without free parameters. At high density in ethane and in $CO_2$, the inverted temperature dependence is not observed, in agreement with theoretical calculations. © 2000 Published by Elsevier Science B.V.

## 1. Introduction

Vibrational relaxation of a solute in a supercritical fluid (SCF) can be studied at fixed temperature as a function of density and at fixed density as a function of temperature [1–3]. Therefore, studies of vibrational relaxation in SCFs provide unique opportunities for investigating relaxation phenomena. Vibrational relaxation, which is highly dependent on the nature of solute–solvent interactions, can also serve as a probe of such interactions in SCFs. Near the critical point, the properties of SCFs change dramatically with temperature and density. Therefore, it is a challenge to incorporate the SCF properties into a theory of vibrational relaxation [1,4].

In this Letter, vibrational relaxation experiments as a function of temperature at constant density, conducted on the asymmetric CO stretching mode of $W(CO)_6$ ($\sim 1990$ cm$^{-1}$), in supercritical ethane and $CO_2$ are compared to theoretical calculations using a recently developed density functional extended hydrodynamic theory of vibrational relaxation. The nature of the temperature dependence of the vibrational relaxation in ethane is unusual [3]. With the density

* Corresponding author. Fax: +1-650-723-4817; e-mail: fayer@fayerlab.stanford.edu; website: fayer2.stanford.edu

0009-2614/00/$ - see front matter © 2000 Published by Elsevier Science B.V.
PII: S0009-2614(00)00682-5

fixed at the critical density ($\rho_c = 6.88$ mol $l^{-1}$), beginning just above the critical temperature ($T_c =$ 305 K, $T_r = 1.006$), as the temperature is increased, $T_1$ becomes longer. $T_1$ continues to increase with increasing temperature until $\sim 70$ K above $T_c$. At still higher temperatures, $T_1$ decreases. In contrast, the lifetime decreases with increasing temperature over the entire range in $CO_2$ at any density or if the density in ethane is raised substantially above $\rho_c$ (12 mol $l^{-1}$).

In several recent studies, the density dependences of vibrational lifetimes of a probe molecule, $W(CO)_6$, in various supercritical fluids (ethane, carbon dioxide, and fluoroform) [1,5] were measured along two isotherms, one at 2 K above the critical temperature ($T_c$), which corresponds to a reduced temperature $T_r \approx 1.006$, and one significantly higher. A hydrodynamic theory of vibrational relaxation of solutes in SCF solvents [6] that was recently extended and made quantitative [1,5], showed very good agreement with the experimental data in ethane and fluoroform and reasonable agreement in carbon dioxide. The purpose of this Letter is to compare theoretical predictions of the temperature dependence of vibrational lifetimes at various fixed densities with experimental data [3].

## 2. Experimental procedures

Infrared vibrational pump–probe experiments (transient absorption measurements) were conducted to measure $T_1$ of the asymmetric stretch of $W(CO)_6$ as a function of temperature at constant density. The experimental procedures have been discussed in considerable detail previously [1]. The doubled output of a mode-locked, Q-switched Nd:YAG laser is used to pump a dye laser. The dye laser output and a 532 nm pulse from the doubled YAG laser pump a $LiIO_3$ OPA. The frequency of the IR OPA is tuned by tuning the dye laser to the peak of the $v = 0 \rightarrow 1$ CO $T_{1u}$ mode absorption of the solute, $W(CO)_6$. The OPA output is $\sim 1$ $\mu$J and has a bandwidth of 0.8 $cm^{-1}$. The pulse duration is $\sim 30$ ps. The frequency, which depends on the temperature and density of the solvent, is $\sim 1990$ $cm^{-1}$. FT-IR spectra were taken of the sample at all temperatures and densities, and the laser was tuned to the peak of the absorption in all cases.

The sample is contained in a high pressure, high temperature cell and sealed with sapphire or calcium fluoride windows [1]. An enclosure was constructed with heaters and fans to produce a uniform temperature. The sample cell, the valves, the pressure transducer, and connecting tubes were all contained within the enclosure, and all were maintained at the same constant temperature within $\pm 0.1$°C. Great care was taken to assure temperature and density uniformity in the SCF sample [1].

## 3. Theory

The theory employs the standard relationship between the vibrational lifetime, $T_1$, and a classical description of the force–force correlation function,

$$k(\rho,T) = T_1^{-1} = \frac{Q}{2m\hbar\omega}\int_{-\infty}^{\infty} \mathrm{d}t \langle F(t)F(0)\rangle_{\mathrm{cl}} \cos(\omega t) \tag{1}$$

where $m$ is the reduced mass of the oscillator and $\omega$ is the Fourier transform frequency associated with energy deposited into the solvent [7]. $Q$ is called the quantum correction factor. $Q$ corrects for the use of the classical force–force correlation functions [8,9].

As discussed in earlier papers [1,6], the force–force correlation function can be determined approximately using the methods of density functional theory. There it was shown that

$$T_1^{-1} \propto Q\int_0^{\infty} \mathrm{d}t \cos(\omega t)\int \mathrm{d}\mathbf{k}\, k^2 \left|\hat{C}_{21}(\mathbf{k})\right|^2 \hat{S}_1(\mathbf{k},t) \tag{2}$$

where $\hat{C}_{21}(\boldsymbol{k})$ is the Fourier transform of the direct correlation function between solute (component 2) and solvent (component 1) and $\hat{S}_1(\mathbf{k},t)$ is the dynamic structure factor of the solvent. Vibrational relaxation has been related to the dynamic structure factor previously [10,11]. The above expression for $T_1$ is particularly useful for investigating vibrational relaxation in SCFs as it permits known density-de-

pendent solvent properties to be used in the calculations of the lifetimes. The proportionality constant, which includes parameters like the oscillator mass, is independent of temperature and density and is neglected.

Eq. (2) contains two $k$-dependent functions, the Fourier transform of the solute–solvent direct correlation function and the dynamic structure factor. A hard sphere direct correlation function is employed. Hard sphere models have proven useful in discussing many aspects of liquids, but they exclude the possibility of solute–solvent attractive interactions. The hard sphere expression derived by Lebowitz [12] yields a direct correlation function dependent on solute and solvent densities and effective hard sphere diameters. It can be used to obtain an exact expression for $\hat{C}_{21}(\boldsymbol{k})$, the form of which has been given previously [1,5].

The dynamic structure factor can be written as the product of the equilibrium static structure factor of the solvent, $\hat{S}_1(\boldsymbol{k})$, multiplied by a time-dependent term. For small wave vectors, this leads to a form that satisfies the Navier–Stokes hydrodynamics equations [13]. The time-dependent piece contains two terms: one that is associated with diffusive motion (Rayleigh peak) and one that describes propagating waves (Brillouin peaks). As discussed in detail previously [1], careful numerical analysis at all wave vectors shows that the calculation of $T_1$ involves large wave vectors only. For large wave vectors, the dynamic structure factor takes the form

$$\hat{S}_1(\mathbf{k},t) = \hat{S}_1(\mathbf{k})\left[\left(1-\frac{1}{\gamma}\right)\mathrm{e}^{-t/\tau_1(k)}\right], \tag{3}$$

where $\hat{S}_1(\boldsymbol{k})$ is approximated by the Ornstein–Zernike expression [13],

$$\hat{S}_1(\mathbf{k}) = \frac{\rho_1 \kappa_\mathrm{T}/\kappa_\mathrm{T}^0}{1+k^2\xi^2} \tag{4}$$

with $\rho_1$ the number density of the solvent, $\kappa_\mathrm{T}$ its isothermal compressibility, $\kappa_\mathrm{T}^0$ is the isothermal compressibility of the ideal gas, $\xi$ is the correlation length of density fluctuations, and $\gamma \equiv C_\mathrm{p}/C_\mathrm{V}$ is the ratio of specific heats.

For the decay constant in the exponential, we employ an expression by Kawasaki [14]

$$\frac{1}{\tau_1(k)} = \frac{k_\mathrm{B}T}{8\pi\eta\xi^3} \times\left[1+k^2\xi^2+\left(k^3\xi^3-\frac{1}{k\xi}\right)\tan^{-1}(k\xi)\right], \tag{5}$$

where $\eta$ is the viscosity. For small $k$, this expression reduces to the hydrodynamic limit $D_\mathrm{T}k^2$, where $D_\mathrm{T}$ is the thermal diffusivity. In the small $k$ limit, the time-dependent factor would contain two terms: a term describing diffusive motion and wave propagation. The single time-dependent term in Eq. (3) is the generalization of the diffusive term to include large $k$. Numerical analysis of $\hat{S}_1(\mathbf{k},t)$ shows that contributions to the $k$ integral in Eq. (2) are overwhelmingly dominated by the function at large $k$, i.e., $k \approx 1\ \text{Å}^{-1}$. The propagating wave term is dropped. It is negligible at large $k$, which is born out by both experiment [15–17] and theory [18,19]. Because the contributions to the $k$ integral in Eq. (2) are sharply peaked at large $k$, the numerical evaluation was carried out for large $k$ only.

The nature of $Q$, the quantum correction factor, is a topic of considerable recent interest [8,9]. The literature shows that one of the better choices [9] is the form put forward by Egelstaff [20]. The Egelstaff correction is given by a prefactor

$$Q = e^{\hbar\omega/2k_\mathrm{B}T}, \tag{6}$$

and the time variable $t$ is replaced as

$$t \to \sqrt{t^2+(\hbar/2k_\mathrm{B}T)^2} \tag{7}$$

in the classical force–force correlation function. The quantum correction factor has a significant effect on the calculated temperature dependence and a small, almost negligible, effect on the density dependence. The time integral can be performed analytically, though the Egelstaff correction factor complicates the final form. A discussion of the functional form of the force–force correlation function that arises from this theory has been given previously [1].

A number of density and temperature-dependent physical parameters are required to evaluate the theoretical expressions. These include $\rho_1$, the number density of the solvent, $\kappa_T$, the isothermal compressibility, $\xi$, the correlation length of density fluctuations, $\gamma \equiv C_p/C_V$, the ratio of specific heats, and $\eta$, the viscosity. Very accurate equations of state and other experimental information provide the necessary input parameters for ethane [21,22] and $CO_2$ [22].

The thermodynamic parameters that enter the theory build in a detailed description of the SCF solvent. All of the input parameters vary substantially with density and temperature. In the near critical region, the variations of the parameters are enormous. In comparing the theory with experiment in the next section, the zero density $T_1$ ($1.28 \pm 0.10$ ns) is removed from the data [23], and the resulting density and temperature-dependent lifetimes, $T_1(\rho,T)$, are compared to the theory. The theoretical curves are scaled to match the data at one particular temperature and density point. The aim is to examine the density and temperature dependences of vibrational relaxation, not the absolute value of the rate of vibrational relaxation.

## 4. Results and discussion

Fig. 1 displays experimental data and theoretical calculations of the density dependence of $T_1(\rho,T)$ data for $W(CO)_6$ in supercritical ethane at 307 K (top curve), which is 2 K above the critical temperature and at 323 K [1]. The solute hard sphere diameter, 6.70 Å, was determined from the crystal structure [24]. Three parameters were varied to obtain the theoretical fit in Fig. 1a. A multiplicative scaling parameter shifts the theoretical curve up and down, but does not change its shape. The theory was scaled to match the data at the critical density, 6.88 mol $l^{-1}$. The solvent hard sphere diameter was varied somewhat, with the optimal value (3.94 Å) being a slight ($\sim 7\%$) reduction from the literature value [25]. The frequency $\omega$ is the parameter that has the major influence on the shape of the calculated curve. It was varied to give the best agreement, which was obtained for $\omega = 150$ $cm^{-1}$. Fig. 1a shows that the theory does a very creditable job of reproducing the density dependence of the data. Fig. 1b displays the 323 K data for the ethane solvent and the theoretically calculated curve. In this calculation the parameters determined by the fit to the data in Fig. 1a are employed; *no further adjustments are made*. As shown by Myers et al., the parameters that go into the calculation change substantially in going from

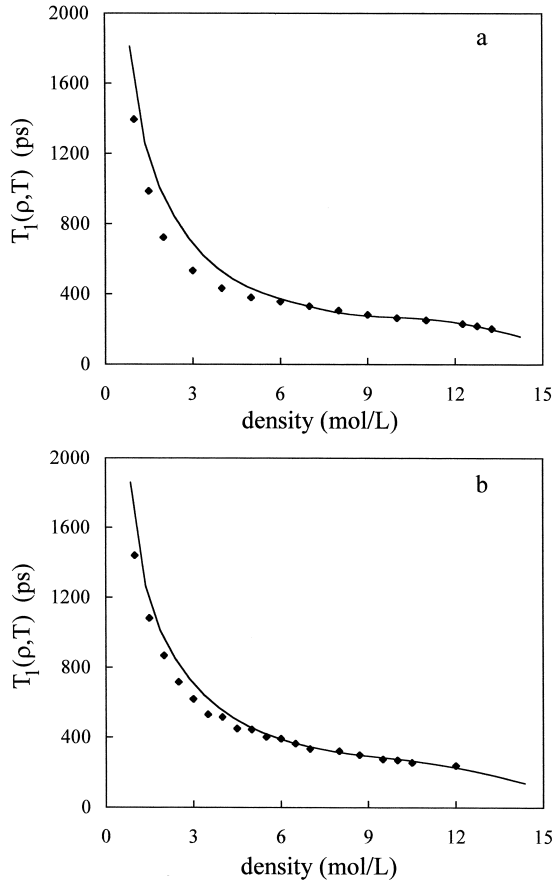


Fig. 1. (a) The density dependence of the vibrational lifetime of the asymmetric CO stretch of $W(CO)_6$ with the zero density contribution removed, $T_1(\rho,T)$, for the solvent ethane at 307 K and the theoretically calculated curve. The theory was scaled to match the data at the critical density, 6.88 mol $l^{-1}$. The best agreement was found for solvent diameter 3.94 Å and $\omega = 150$ $cm^{-1}$, the energy deposited directly into the solvent upon relaxation. (b) $T_1(\rho,T)$ versus density for the solvent ethane at 323 K and the theoretically calculated curve $T_1(^{\rho},T)$. The scaling factor, frequency $\omega$, and the hard sphere diameters are the same as those used in the fit of the 307 K data. The agreement is very good without free parameters.

307 K (near critical temperature) to 323 K [1]. Nonetheless, the theory is able to reproduce the data, and the agreement is very good given the lack of free parameters.

The calculations are quite sensitive to the choice of $\omega$. It was found that the same value of $\omega$ gave the best agreement with the data in ethane, fluoroform, and $CO_2$. The fact that the same $\omega$ arises in the fits to data in all three solvents suggests that this is not an arbitrary value, but rather reflects the energy deposited into the solvent in the course of the vibrational relaxation. Calculations were also performed in which a distribution of $\omega$ was used [1]. It is found that $\omega$ need not be a single frequency to produce the curves shown in Fig. 1. For instance, relaxation times calculated by averaging over a Gaussian distribution of frequencies with a 150 $cm^{-1}$ mean and a standard deviation of 20 $cm^{-1}$ are identical to the results shown in the figures. This frequency is most likely located in the single 'phonon' density of states (DOS) of the continuum of low frequency modes of the solvents. Instantaneous normal mode calculations in $CCl_4$, $CHCl_3$, and $CS_2$ show cut-offs in the DOS at $\sim 150$ $cm^{-1}$, $\sim 180$ $cm^{-1}$, and $\sim 200$ $cm^{-1}$, respectively [26,27]. The higher frequency portions of the DOS are dominated by orientational modes. Since ethane, fluoroform and $CO_2$ are much lighter than the liquids cited above, it is expected that their DOS will extend to higher frequency.

Standard theories of vibrational relaxation [7,28] take a variety of approaches. However, one almost universal trait is that the vibrational lifetime of an oscillator decreases with an increase in temperature at constant density. In the simplest isolated collision theories [7], as one increases the temperature of a system at fixed density, the collision frequency will increase leading to faster relaxation. (This assumes that the collision diameters of the particles do not change significantly [25,29]

Fig. 2 shows the vibrational lifetime $T_1(\rho,T)$ as a function of temperature in ethane at the critical density (6.88 mol $l^{-1}$). Between 307 K and $\sim 375$ K, as the temperature increases the lifetime becomes longer. We refer to this temperature dependence as inverted. Above $\sim 375$ K, the lifetime decreases with further increases in temperature. An inverted temperature dependence in vibrational relaxation has been observed in a few liquid systems

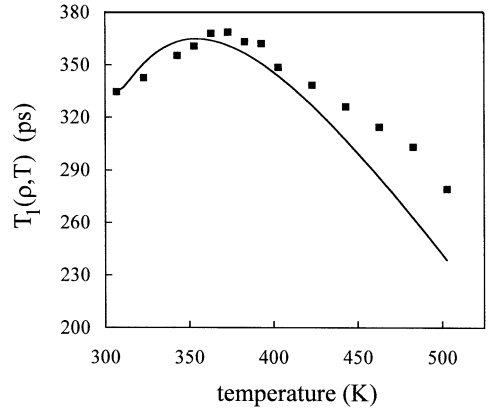


Fig. 2. The temperature dependence of the vibrational lifetime of the asymmetric CO stretch of $W(CO)_6$ with the zero density contribution removed, $T_1(\rho,T)$, for the solvent ethane at fixed density, the critical density, $\rho_c = 6.88$ mol $l^{-1}$, and the theoretically calculated curve. Note the presence of an inverted temperature regime, i.e., the lifetime initially becomes slower as the temperature is increased. The theoretical calculation uses the parameters obtained from the density dependence (Fig. 1a) without further adjustment. The theory does a very respectable job of predicting the shape, including a near quantitative match with the amplitude and temperature at the maximum. At higher temperatures the calculated slope drops somewhat faster than the data. (The scale is greatly expanded relative to Fig. 1.)

[30,31], but in liquids, as the temperature is increased the density of the liquid decreases. There is a trade trade-off in liquids between increasing temperature and decreasing density that can influence the form of the temperature dependence [27]. The behavior of the vibrational relaxation in water near its freezing point is probably caused by changes in hydrogen bonding that occur near the phase transition [31]. The mechanisms responsible for inverted temperature dependences in liquids do not occur at fixed density.

The calculated temperature-dependent curve in Fig. 2 was obtained using known solvent parameters at each temperature and the parameters determined by the fit to the density-dependent data in Fig. 1a, without adjustment. Thus, there are no free parameters in the calculation. While the agreement between the calculation and the data is not perfect, the calculation does a good job of capturing the essential features of the data. The theory predicts the existence of the inverted region, and matches nearly quantita-

tively the amplitude and temperature at which the lifetime reaches a maximum. However, the theoretical curve drops too rapidly with temperature above $\sim 400$ K.

At densities below and somewhat above the critical density, the data are still inverted [3]. However, at sufficiently high density, the data do not display an inverted region. Fig. 3 shows temperature-dependent data at 12 mol $l^{-1}$. The solid line is the calculated curve using the temperature-dependent solvent parameters at 12 mol $l^{-1}$ and the parameters determined from the density-dependent data in Fig. 1a. While the agreement is not quantitative, the most important feature, the lack of an inverted temperature dependence, is reproduced. Furthermore, changing from the critical density (6.88 mol $l^{-1}$) to 12 mol $l^{-1}$ drastically changes all of the input parameters to the theory. Given the lack of free parameters, the theory does a respectable job of reproducing the data.

Fig. 4 displays $T_1(\rho,T)$ data as a function of temperature in $CO_2$ at the critical density (10.6 mol $l^{-1}$). The data do not display an inverted temperature dependence at the critical density or any other density investigated [3]. The solid line is the theoretical calculation, using parameters obtained from fitting the $CO_2$ density dependence (fixed temperature, $T=306$ K) (solute diameter $=6.70$ Å, solvent diameter $=3.60$ Å, and frequency $\omega=150$ cm$^{-1}$) [1]. Like the data, the calculation does not have an inverted region, although there is a change in slope at low temperature. Again, the theory is able to capture the essential nature of the temperature-dependent data without free parameters.

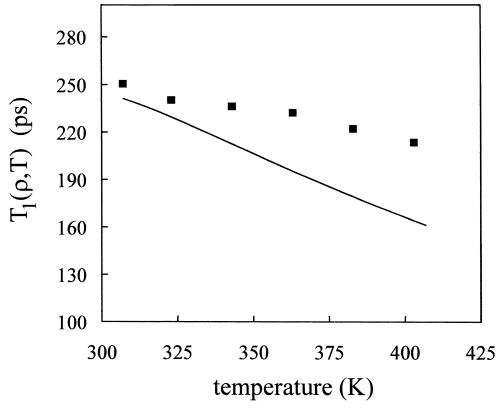


Fig. 3. $T_1(\rho,T)$ versus temperature for the solvent ethane along the 12 mol $l^{-1}$ isochore. The data no longer show an inverted temperature dependence. The theory, with no free parameters, captures the essential feature of the data, the lack of an inverted temperature regime, though it overestimates the slope. (The scale is greatly expanded relative to Fig. 1.)

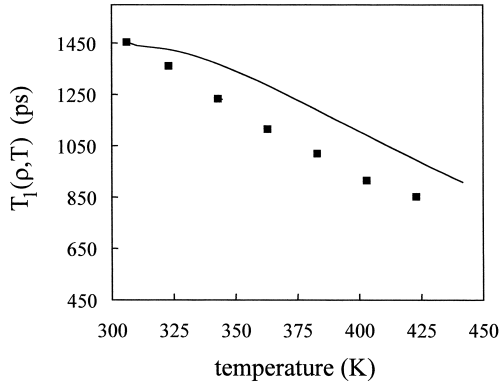


Fig. 4. $T_1(\rho,T)$ versus temperature for the solvent carbon dioxide along the critical isochore ($\rho_c=10.6$ mol $l^{-1}$). Unlike the temperature dependence in ethane (Fig. 2), the temperature dependence in $CO_2$ at the critical density does not have an inverted region. The theory properly displays the lack of an inverted temperature region, and, away from the critical temperature, has approximately the correct slope. (The scale is greatly expanded relative to Fig. 1.)

## 5. Concluding remarks

In this Letter, the the extended hydrodynamic theory of vibrational relaxation in SCFs was compared to measurements of the temperature-dependent lifetime of the asymmetric CO stretch of $W(CO)_6$ in ethane and $CO_2$. The theory, which was shown previously to be able to describe the density dependence of $T_1$ at fixed temperature [1], does a good job of reproducing the temperature dependence without free parameters. In particular, the inverted temperature dependence observed in ethane at the critical density is reproduced nearly quantitatively and the lack of inverted temperature dependences in high density ethane and in $CO_2$ are also reproduced.

Egorov and Skinner have used a theory that involves Lennard-Jones (LJ) spheres and a breathing sphere model to calculate the density and temperature dependence [4] of some of the data presented here and previously [1]. By adjusting a number of parameters, including the LJ parameters, their theory is able to reproduce the density-dependent data in ethane and the temperature-dependent data in ethane at the critical density only. The agreement of the Egorov–Skinner theory with the data is comparable to that obtained with the hydrodynamic theory. It is not known if the Egorov–Skinner theory can reproduce the lack of an inverted region at high density in ethane or at all densities in $CO_2$. Their calculations involve mild solute–solvent clustering.

The extended hydrodynamic theory discussed here contains important details of the solvent by employing a variety of the solvent's hydrodynamic and thermodynamic properties as input parameters. The spatial distribution of the solvent about the solute comes in through the Fourier transform of the solute–solvent direct correlation function, $\hat{C}_{21}(\boldsymbol{k})$. The fluid's $\hat{C}_{21}(\boldsymbol{k})$ is approximated using an exact hard sphere expression. The fact that the theory can reproduce the observed diverse temperature and density trends [1,5] suggests that the theory is capturing the essential features of vibrational energy relaxation. Using a hard sphere $\hat{C}_{21}(\boldsymbol{k})$ means that the theory does not involve solute–solvent attractive interactions that could give rise to local density enhancement of the solvent around the solute (clustering) [32–34]. Such attractive clustering is distinct from local density augmentation that can arise from critical phenomena [35]. Clustering arising from specific solute–solvent attractive interactions has been invoked to explain a variety of experimental observables [32–34]. The results presented here and previously [1] indicate that even near the critical point, observables measured in SCFs may not require solute–solvent clustering as part of their explanation. Critical phenomena can be important, and they are brought into the extended hydrodynamic theory via the input of detailed solvent parameters. The properties of an SCF solute–solvent system change substantially as the system is moved away from the critical point. The theory presented above can reproduce substantial features of vibrational relaxation in the systems studied.

## Acknowledgements

D.J.M. thanks the Stanford University Lieberman Fund for a graduate fellowship. M.S. thanks the Mitsubishi Chemical Corporation for financial support. This work was supported by the AFOSR (Grant No. F49620-94-1-0141).

## References

[1] D.J. Myers, M. Shigeiwa, B.J. Cherayil, M.D. Fayer, J. Phys. Chem. B 104 (2000) 2402.
[2] R.S. Urdahl, D.J. Myers, K.D. Rector, P.H. Davis, B.J. Cherayil, M.D. Fayer, J. Chem. Phys. 107 (1997) 3747.
[3] D.J. Myers, S. Chen, M. Shigeiwa, B.J. Cherayil, M.D. Fayer, J. Chem. Phys. 109 (1998) 5971.
[4] S.A. Egorov, J.L. Skinner, J. Chem. Phys. 112 (2000) 275.
[5] D.J. Myers, M. Shigeiwa, B.J. Cherayil, M.D. Fayer, Chem. Phys. Lett. 313 (1999) 592.
[6] B.J. Cherayil, M.D. Fayer, J. Chem. Phys. 107 (1997) 7642.
[7] D.W. Oxtoby, Ann. Rev. Phys. Chem. 32 (1981) 77.
[8] S. Egorov, B. Berne, J. Chem. Phys. 107 (1997) 6050.
[9] S.A. Egorov, K.F. Everitt, J.L. Skinner, J. Phys. Chem. A 103 (1999) 9494.
[10] V.B. Nemtsov, I.I. Fedchenia, A.V. Kondratenko, J. Schroeder, Phys. Rev. E 60 (1999) 3814.
[11] B.P. Hills, Mol. Phys. 35 (1978) 1471.
[12] J.L. Lebowitz, Phys. Rev. 133 (1964) 895.
[13] H.E. Stanley, Introduction to Phase Transitions and Critical Phenomena, Oxford, New York, 1971.
[14] K. Kawasaki, Ann. Phys. 61 (1970) 1.
[15] T.A. Postol, C.A. Pelizzari, Phys. Rev. A 18 (1978) 2321.
[16] I.M. de Schepper, P. Verkerk, A.A. van Well, L.A. de Graaf, Phys. Rev. Lett. 50 (1983) 974.
[17] I.M. de Schepper, E.G.D. Cohen, Phys. Rev. A 22 (1980) 287.
[18] W.E. Alley, B.J. Alder, Phys. Rev. A 27 (1983) 3158.
[19] W.E. Alley, B.J. Alder, S. Yip, Phys. Rev. A 27 (1983) 3174.
[20] P.A. Egelstaff, Adv. Phys. 11 (1962) 203.
[21] B.A. Younglove, J.F. Ely, J. Phys. Chem. Ref. Data 16 (1987) 543.
[22] N.I. of Standards, US Department of Commerce, Boulder, CO, 1992.
[23] D.J. Myers, M. Shigeiwa, R.J. Silbey, M.D. Fayer, Chem. Phys. Lett. 312 (1999) 399.
[24] F. Heinemann, H. Schmidt, K. Peters, D. Thiery, Z. Kristallogr. 198 (1992) 123.
[25] D. Ben-Amotz, D.R. Herschbach, J. Phys. Chem. 94 (1990) 1038.
[26] P.B. Moore, X. Ji, H. Ahlborn, B. Space, Chem. Phys. Lett. 296 (1998) 259.
[27] P. Moore, A. Tokmakoff, T. Keyes, M.D. Fayer, J. Chem. Phys. 103 (1995) 3325.

[28] J. Chesnoy, G.M. Gale, Ann. Phys. Fr. 9 (1984) 893.
[29] J. DeZwaan, R.J. Finney, J. Jonas, J. Chem. Phys. 60 (1974) 3223.
[30] A. Tokmakoff, B. Sauter, M.D. Fayer, J. Chem. Phys. 100 (1994) 9035.
[31] S. Woutersen, U. Emmerichs, H.-K. Nienhuys, H.J. Bakker, Phys. Rev. Lett. 81 (1998) 1106.
[32] O. Kajimoto, Chem. Rev. 99 (1999) 355.
[33] S. Kim, K.P. Johnston, AIChE J. 33 (1987) 1603.
[34] S. Kim, K.P. Johnston, Ind. Eng. Chem. Res. 26 (1987) 1206.
[35] S.C. Tucker, Chem. Rev. 99 (1999) 391.